Structural Engineering and Mechanics, Vol. 20, No. 6 (2005) 673-693
DOI: http://dx.doi.org/10.12989/sem.2005.20.6.673

Long-term behavior of segmentally-erected prestressed concrete box-girder bridges

S. Hedjazi† and A. Rahai‡

Department of Civil and Environmental Engineering, Amirkabir University, Tehran, Iran

K. Sennah‡†

Civil Engineering Department, Ryerson University, Toronto, Ontario, Canada

(Received October 13, 2004, Accepted May 17, 2005)

Abstract. A general step-by-step simulation for the time-dependent analysis of segmentally-erected prestressed concrete box-girder bridges is presented. A three dimensional finite-element model for the balanced-cantilever construction of segmental bridges, including effects of the load history, material nonlinearity, creep, shrinkage, and aging of concrete and the relaxation of prestressing steel was developed using ABAQUS software. The models included three-dimensional shell elements to model the box-girder walls and Rebar elements representing the prestressing tendons. The step-by-step procedure allows simulating the construction stages, effects of time-dependent deformations of materials and changes in the structural system of the bridges. The structural responses during construction and throughout the service life were traced. A comparison of the developed computer simulation with available experimental results was conducted and good agreement was found. Deflection of the bridge deck, changes in stresses and strains and the redistribution of internal forces were calculated for different examples of bridges, built by the balanced-cantilever method, over thirty-year duration. Significant time-dependent effects on the bridge deflections and redistribution of internal forces and stresses were observed. The ultimate load carrying capacities of the bridges and the behavior before collapse were also determined. It was observed that the ultimate load carrying capacity of such bridges decreases with time as a result of time-dependent effects.

Key words: segmental bridges; box-girder; prestress; long-term deformations; time-dependent analysis; balanced-cantilever construction; redistribution of stresses; ultimate load.

1. Introduction

Segmental construction of prestressed, reinforced and composite concrete and steel structures is a common trend for today's structures and bridges. The study of the influence of the construction process, short-term and long-term effects caused by time-dependent deformations of materials and changes in the structural systems are usually of great importance. One of the most interested construction methods for prestressed concrete box-girder bridges, is the balanced-cantilever

† Ph.D. Candidate
‡ Associate Professor
‡† Associate Professor, Corresponding author, E-mail: ksennah@ryerson.ca

construction technique. The balanced-cantilever construction of prestressed concrete box-girder bridges has been recognized as one of the most efficient methods of bridge construction. This method has great advantages over other methods, especially in urban areas where traffic may be interrupted, or over deep valleys or waterways where false work could be expensive and hazardous. Erecting segmental concrete bridges with the balanced-cantilever method may lead to longer spans with less cost and time of construction. In this method, segments of the bridge superstructure are assembled in an appropriate sequence as cantilevers on opposite sides of the bridge pier. When the cantilevers from adjacent piers meet, they can be jointed together by hinges or by post-tensioned continuity cables. Utilization of continuity cables causes reduction of bridge deflection and better resisting moments due to superimposed loads and also those loads which develop gradually with time.

As the construction progresses, the statically determinate structure changes to a statically indeterminate one, which should be considered in the design process. Precast or cast-in-place segments can be assembled using a post-tensioning technique. During the construction stages and also in service life, time-dependent deformations of materials proved to have significant effects on the behavior of the bridge. So, a realistic consideration of material properties, including time-dependent structural effects due to creep and shrinkage of concrete, relaxation of prestressing steel and changing of concrete properties with time, is necessary at all different ages and stages of construction and during the service life of the bridge superstructure. Few examples of time-dependent effects which have resulted in poor surface conditions, cracking, poor serviceability and loss in durability, were recorded in the literature. The Yuan-Shan highway bridge located in Taipei city of Taiwan, which was constructed by the balanced-cantilever method, has a recent recorded vertical deflection of about 600 mm at the mid-span hinged connection (Chiu *et al.* 1996). The Quebec Highway Fifteen's twin bridges, built using cast-in-place concrete box girder segments with the cantilever technique, is another example of this type of bridges that was made continuous at the mid-span. However, large mid-span deflections, together with web and slab's cracks and opening of joints between segments resulting from extensive tensile stress zones, caused them to be strengthened (Ouellet and Gaumond 1990).

During the last few decades, few simplified models for instantaneous and time-dependent analysis of segmental bridges have been proposed. Most of these studies considered planar and elastic behavior of structures (Tadros *et al.* 1979, Ketchum and Scordelis 1986, Bishara and Papakonstantinou 1990, Elbadry and Debaiky 1998), while very few dealt with simplified techniques for nonlinear properties of materials (Kang and Scordelis 1990, Cruz *et al.* 1998). In other studies, prestressing cables were ignored or their effects were considered as equivalent nodal forces (Shashkewich 1986, Chiu *et al.* 1996). Many of the time-dependant analysis models were developed for specific bridge types, such as cable-stayed bridges and bridges built by incremental launching or by span-by-span technique (Vanzyl and Scordelis 1979). Other studies dealt with composite steel box girder bridges including stages of slab casting and time-dependent nonlinear analysis (Kwak *et al.* 2000, Mari 2000, Mari *et al.* 2003). Statically determinate bridges built by the balanced-cantilever method were discussed elsewhere (Danon and Gamble, 1977, Chiu *et al.* 1996). Comparisons between analytical results for time-dependent deformations of materials and some responses from structures were also reported (Russell *et al.* 1982, Melby *et al.* 1996, Robertson 1998, Santos *et al.* 2001, Takacs and Kanstad 2001). Few authors investigated the effects of creep and shrinkage on prestressed and concrete structures (Bazant 1972, Dilger 1982, Ghali and Elbadry 1989, Gwozdziewicz *et al.* 2000). Others conducted sensitivity analysis on the ACI-209 (1992) or CEB-FIP (1978 and 1990) models for time-dependent effects on structural performance (Bellevue

and Towell 2000, Oh and Yang 2000, Lefebvre 2002). Finally, some studies (Floris *et al*. 1991, Dezi and Tarantino 1991, Kwak and Son 2002) have been performed to introduce simple equations or graphs, considering a change in structural system and creep effects, to be used for design purposes, but according to numerous simplifying assumptions, they could not be used in real conditions or in practice, given the fact that some does not give accurate results for the situations other than the assumed ones.

In the present paper, a general step-by-step simulation for the time-dependent analysis of segmental prestressed concrete box-girder bridges is presented, which takes into account time-dependent effects, construction stages and realistic material properties. The proposed procedure, which is used for bridges built by the balanced-cantilever technique, allows the designer to determine the effects of the construction process, short-term and long-term effects and changes in the structural system from statically determinate to a statically indeterminate, on the bridge structural behavior. Two examples of bridge prototypes were simulated using the finite-element method and their structural behavior up to thirty years after construction was determined and has been presented in this paper. Also, the ultimate load carrying capacity of these bridge prototypes, when subjected to truck loading, was also evaluated by taking into account both material and geometric nonlinearity.

2. Description of the finite-element modelling

The general purpose finite-element "ABAQUS" software (Hibbitt *et al*. 2004) is used for the numerical simulation of a segmental bridge built by the balanced-cantilever construction technique. A data deck for this program contains model data and history data. The model data define the finite-element model such as elements, nodes, element properties, material definitions and boundary conditions, while the history data define the sequence of loading and the response of the structure. This history is divided into a sequence of steps, so a step-by-step procedure is used for different construction stages and ages of the bridge superstructure. Each bridge segment is assembled in a different step, in which long-term deformations of materials are considered for the period up to assemblage of the next bridge segment in a following step. Changes in concrete elastic modulus with time, creep, and shrinkage of concrete and relaxation of prestressing steel is considered in the time-dependent analysis. It should be noted that the deformed shape of the bridge segments in each construction step, resulting from the ABAQUS analysis, is considered as an initial geometry of the constructed bridge segment in the following construction step. This is achieved by adding a soft auxiliary mesh that adjusts the nodal coordinates of the next segment due to assemblage and deformations of previous segments. Three-Dimensional Shell elements, S4R, are selected to simulate the bridge deck slab, webs and bottom flange. To facilitate modelling the arbitrary geometry for prestressing cables and tendons in the shell elements, "Rebar" option in ABAQUS is used. Initial Conditions are used to define the prestress in the Rebar, as prestressing cables. In modelling the prestressing forces, instantaneous losses due to anchorage slip, friction, and elastic shortening are considered in each construction stage. The PRESTRESSHOLD option in the ABAQUS software is utilized to model the post-tensioning process. It ha been mentioned earlier that in the time-dependent analysis of the structure, the time domain is divided into a discrete number of steps. At each time step, the structure is analyzed under the external applied loads and the initial conditions for this step are the results from the previous steps.

2.1 Modelling of instantaneous material behavior

The concrete model in ABAQUS is designed to provide a general capability for modelling plane, reinforced and prestressed concrete. The "Rebar" is a one-dimensional strain theory element which may be used with standard metal plasticity models to describe the behavior of "Rebar" material. The situation at the interface of rebar and concrete is modelled by introducing the "Tension Stiffening" which is used to simulate load transfer across cracks through the "Rebar". The model is a smeared crack model, and it does not simuate individual "macro" cracks. The response of cracks is entered into the calculations at each integration point by the way in which the cracks effect the stress and material stiffness associated with the integration point. The instantaneous stress-strain curve for the concrete under compression is of a parabolic-linear type, with a descending branch, unloading and reloading. In tension, a linear branch up to cracking and a descending hyperbolic curve at post-cracking are considered in order to take into account the tension stiffening and the possibility of reloading after the closing of the crack. The cracking and compressive response of concrete that are incorporated in the model are illustrated by the uniaxial response of a specimen in Fig. 1(a).

The concrete initially exhibits elastic response when it is loaded in compression. Some non-recoverable straining occurs as the stress is increased and the response of material softens. A uniaxial concrete specimen responds elastically when in tension until at a stress, which is typically seven to ten percent of the ultimate compressive stress, is reached. Then, cracks form. Cracks are modelled in ABAQUS as strain softening. In multiaxial stress states, the previous observations are generalized through the concept of surfaces of failure. Briefly, when the strain of concrete reaches the tensile strain corresponding to tensile strength, cracking takes place. Now the influence of tension stiffening for the concrete in tension causes the tensile stress not to drop to zero, but it gradually decreases as the tensile strain increases, according to Fig. 1(a). Such procedure is implemented taking into account reloading and unloading processes (Hibbitt *et al.* 2004). In the present study, reinforcing and prestressing steel are assumed to be a linear elastic-perfect plastic

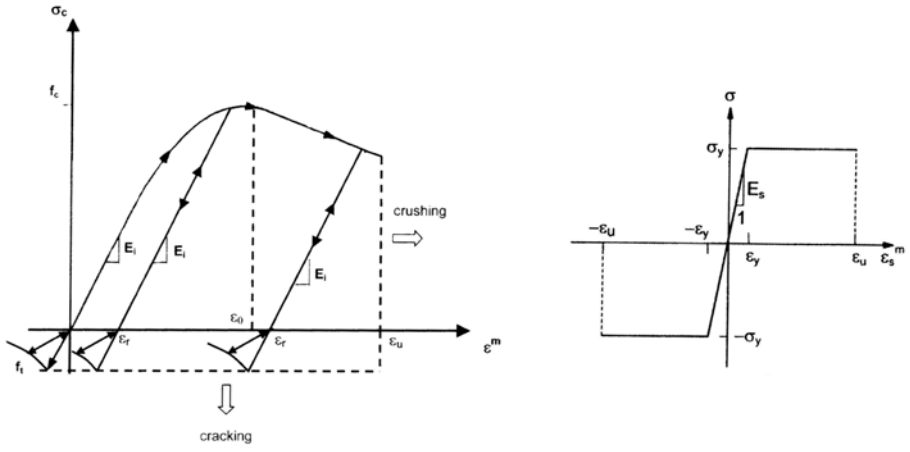

(a) Concrete (b) Steel

Fig. 1 Stress-strain relations of constitutive material

material with a stress-strain relation shown in Fig. 1(b). Bilinear and multi-linear stress-strain relationships are applicable in ABAQUS software when required.

2.2 Modelling of time-dependent material

Segmental construction techniques, such as the balanced-cantilever technique type require accurate simulation of the time-dependent behavior of the bridge superstructure during either the construction and operating stages. Time-dependent deformations of materials which cause considerable effects on the short-term and long-term behaviour of the bridge consist of creep, shrinkage, change in properties of concrete and relaxation of prestressing steel. Prestressing cables, which are modelled as "Rebar" elements and with specific initial conditions to apply prestress, use the same nodes as other shell elements and contribute to the global stiffness matrix. Every arbitrary geometry, including curved cables, and material properties for these cables are applicable. Relaxation of prestressing steel is calculated as follows and is applied as nodal forces as recommended elsewhere (ACI 209, 1992).

$$f_p = f_{pi}\left[1 - \frac{Logt}{10}\left(\frac{f_{pi}}{f_{py}} - 0.55\right)\right] \tag{1}$$

Where f_{py} and f_{pi} are the yield and initial stresses of the prestressing steel, respectively; f_p is the prestressing steel stress at time t.

After the concrete is placed, time-dependent effects due to creep and shrinkage occur with the aging of concrete. Shrinkage strain can be evaluated directly by utilizing the shrinkage model proposed by the American Concrete Institute (ACI 209, 1992) as the volume change, which occurs independently of imposed stresses. Assuming that the non-prestressing steel is uniformly distributed over the bridge cross-section, then the effect of shrinkage on deformations would be limited to its time effect on prestress losses only (Bishara and Papakonstantinou 1990), and shrinkage is treated in the same way as prestressing losses with time. Shrinkage of concrete is considered as follows in each time step.

$$\varepsilon_s(t, t_0) = \left[\frac{t - t_0}{35 + (t - t_0)}\right]\varepsilon_{s\infty} \tag{2}$$

$$\varepsilon_{S\infty} = 780 \times 10^{-6}\ \beta_1'\beta_2'\beta_3'\beta_4'\beta_5'\beta_6'\beta_7' \tag{3}$$

Where $\varepsilon_{S\infty}$ is ultimate shrinkage strain, $\varepsilon_{s(t, t0)}$ is shrinkage strain of concrete at any time t, t_0 is age of concrete at the end of initial wet curing and $\beta_i'(i = 1, 2, ...)$ represent the applicable correction factors for different conditions (ACI 209, 1992).

Concrete is a material that exhibits creep and also its properties change considerably with time. Hence, the modulus of elasticity and the creep function of concrete should be replaced by the time-dependent equivalents in computing the structure stiffness matrix. During the construction process, a particular segment is loaded incrementally at different ages. With each age corresponding to the time, a new segment is added to the system. Also, during the service time, internal forces change with time because of time-dependent effects. Thus, to predict the effects of creep and aging of concrete, the Trost-Bazant Method for creep analysis is used. This method, which is called Age Adjusted Effective Modulus Method, introduces the concept of an "aging" coefficient (Neville *et al.*

1983). This coefficient used to be referred to as a Relaxation coefficient. Both names have their justifications, but in order to avoid confusion with the computation of prestress losses, where relaxation of prestressing steel plays a role, the term "aging" coefficient has been used. As the integral equation for creep analysis in the state of changing stresses can not be solved in closed form, when the creep or flow curves are non-parallel, the aging coefficient concept has been developed. More details are presented elsewhere (Neville *et al.* 1983, ACI 209, 1992). The aging coefficient accounts for the effect of aging on the ultimate value of creep for stress increments or decrements occurring gradually after application of original loads, and is defined by the following equation.

$$\chi(t, t_0) = \frac{E(t_0)}{\phi(t, t_0)[\sigma_{(t)} - \sigma_{(t_0)}]} \int_0^t \frac{1 + \phi(t, t')}{E(t')} \times \frac{\partial \sigma(t')}{\partial t'} dt' - \frac{1}{\phi(t, t')} \tag{4}$$

$$\chi(t, t_0) = \frac{E(t_0)}{\phi(t, t_0)[\sigma_{(t)} - \sigma_{(t_0)}]} \sum_{t_0}^{t} \frac{\Delta \sigma(t')}{E(t')} \times [1 + \phi(t, t')] - \frac{1}{\phi(t, t_0)} \tag{5}$$

Where $\chi(t, t_0)$ is the aging coefficient, E is modulus of elasticity of concrete at different ages, σ is stress at different ages, $\phi(t, t_0)$ is the creep coefficient at any time, t (days), for concrete loaded at the age, t_0, and t' is age of concrete at the application of variable loads.

The age-adjusted elastic and shear modulus values of concrete, E_{ca} and G_{ca}, respectively, which are used in the elasticity matrix are replaced by the age-adjusted values given by:

$$E_{ca}(t_{k+1}, t_k) = E_c(t_k)/[1 + \chi\phi(t_{k+1}, t_k)] \tag{6}$$

$$G_{ca}(t_{k+1}, t_k) = E_{ca}(t_{k+1}, t_k)/[2(1 + \nu)] \tag{7}$$

Where χ is the same as $\chi(t, t_0)$, and $\phi(t_{k+1}, t_k)$ is creep coefficient in the period of (t_{k+1}, t_k), and ν is Poisson's ratio, during the interval k. The value of χ is usually close to 0.8 and for practical implementation on bridge, the value of 0.82 is recommended (Elbadry and Debaiky 1998, Neville *et al.* 1983). The creep coefficient, $\phi(t, t_0)$, modulus of elasticity and compressive strength of concrete with time can be calculated as follows:

$$\phi(t, t_0) = \left[\frac{(t - t_0)^{0.6}}{10 + (t - t_0)^{0.6}}\right] \phi_\infty \tag{8}$$

$$\phi_\infty = 2.35\beta_1.\beta_2.\beta_3.\beta_4.\beta_5.\beta_6 \tag{9}$$

$$E_c(t) = 0.043\sqrt{\rho^3 f_c'(t)} \tag{10}$$

$$f_c'(t) = \frac{t}{a + bt} f_{c28}' \tag{11}$$

Where ϕ_∞ is ultimate creep coefficient of concrete. ρ, $f_c'(t)$, and f_{c28}' are unit weight of concrete, compressive strength of concrete at any time t, and at 28 days, respectively. β_i ($i = 1, 2, ...$), a and b are represented by the applicable correction factors for different conditions (ACI 209, 1992).

2.3 Effects of different construction stages

Each balanced-cantilever consists of a number of box-girder segments. Different loads, such as segment's weight and prestressing, introduce time-dependent effects on the system when a segment is placed. Therefore, several time intervals for different stages of construction and time-dependent effects have to be adopted, and the analysis is repeated at these small intervals. The results of each time intervals are added to previous results. The same procedure is followed by the subsequent segments. At each step and each construction stage, the deflections and stresses are available in the ABAQUS output file. The continuity of the bridge is achieved after casting the closure segment and the post-tensioning of continuity tendons. At this stage, the structural system changes from statically determinate to statically indeterminate. Therefore, internal forces in the continuous system are produced by the long-term effects of girder weight, prestressing forces and superimposed loads (i.e., weight of the sidewalk and covering materials). It is obvious that displacements that would have continued to take place in the statically determinate system due to shrinkage, creep and relaxation, become restrained by imposed boundary conditions of the completed structure (Fig. 2). This phenomenon, which induces additional internal forces, is known as the redistribution of internal forces. The change in the structural system of the bridge superstructure from statically determinate to indeterminate was simulated in ABAQUS software in a separate step and by changing the boundary conditions to "Fixed" supports. The superimposed loads and continuity cables are applied in to subsequent steps after the closing step.

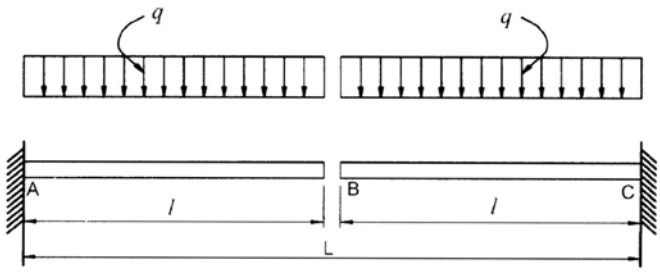

(a) Configuration of cantilever

(b) Elastic deformations in a cantilever

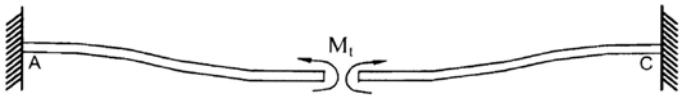

(c) Restraint moment M_t after closure

Fig. 2 Deformation and distribution of internal forces before and after closure

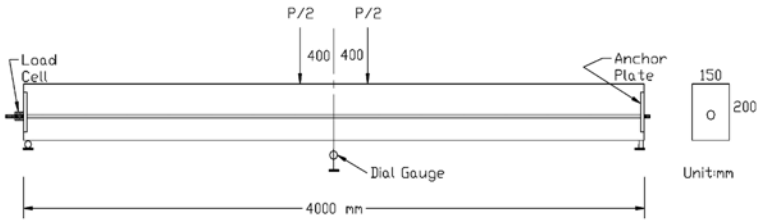

Fig. 3 Flexural test set up (quoted from Chiu *et al.* 1996)

3. Experimental verifcation of the approach

To examine the accuracy of the time-dependent analysis performed by the ABAQUS software and the simulation of creep and shrinkage of concrete and relaxation of prestressing steel, several experimental tests on simply-support beams conducted at Taiwan University (Chiu *et al.* 1996) are selected. These tests were performed on six laboratory-scale prestressed concrete beams to investigate their behavior under the effects of long-term deformation of materials. Fig. 3 shows the test set up and beam dimensions. The prestress tendons which have been used were high tension and low relaxation strands with a 12.8 mm diameter. More details can found elsewhere (Chiu *et al.* 1996). The experimental results consist of three different tests. All the specimens were subjected to the self weight of the beam, superimposed load, P, of 2835 N, and prestressing forces with an initial prestress force close to 100 kN. The first and third specimens (SB13B and SB17B, respectively) were subjected to all the time-dependent deformations of materials including creep and shrinkage of concrete and relaxation of prestressing steel. While, the second specimen (SB13C) was sealed with siliconized acrylic latex caulk to prevent the moisture loss from beam to simulate the basic creep condition and without the effect of drying shrinkage. The first and second specimens (SB13B and SB13C, respectively) were tested under the same loading age of three days, while the third one was loaded at the age of seven days. Creep, shrinkage, change of modulus of elasticity of concrete with time and relaxation of prestressing steel are modelled as instructed earlier in this paper. Beam elements with prestressing cables are used to model the tested beams. The comparison between the analytical results and the experimental findings is shown in Fig. 4. The experimental results are compared with the results obtained from the different analysis options including (i) only creep effect, (ii) both creep and relaxation effects, and (iii) creep, shrinkage and relaxation effects all together. Good agreement is observed, especially when considering the combined effects of creep and shrinkage of concrete and the relaxation of prestressing steel.

4. Numerical examples

Examples of realistic prestressed concrete box-girder bridges segmentally-erected using the balanced-cantilever technique are discussed to demonstrate their long-term behaviour. Two straight multi-span bridges (MSB1 and MSB2) built by the balanced-cantilever technique (Ketchum and Scordelis 1986) are considered and have been analyzed using ABAQUS software. The structural behavior of the bridges under dead load and prestressing are traced through the construction phase and thirty-year following period. The effects of live load at the end of construction and different age

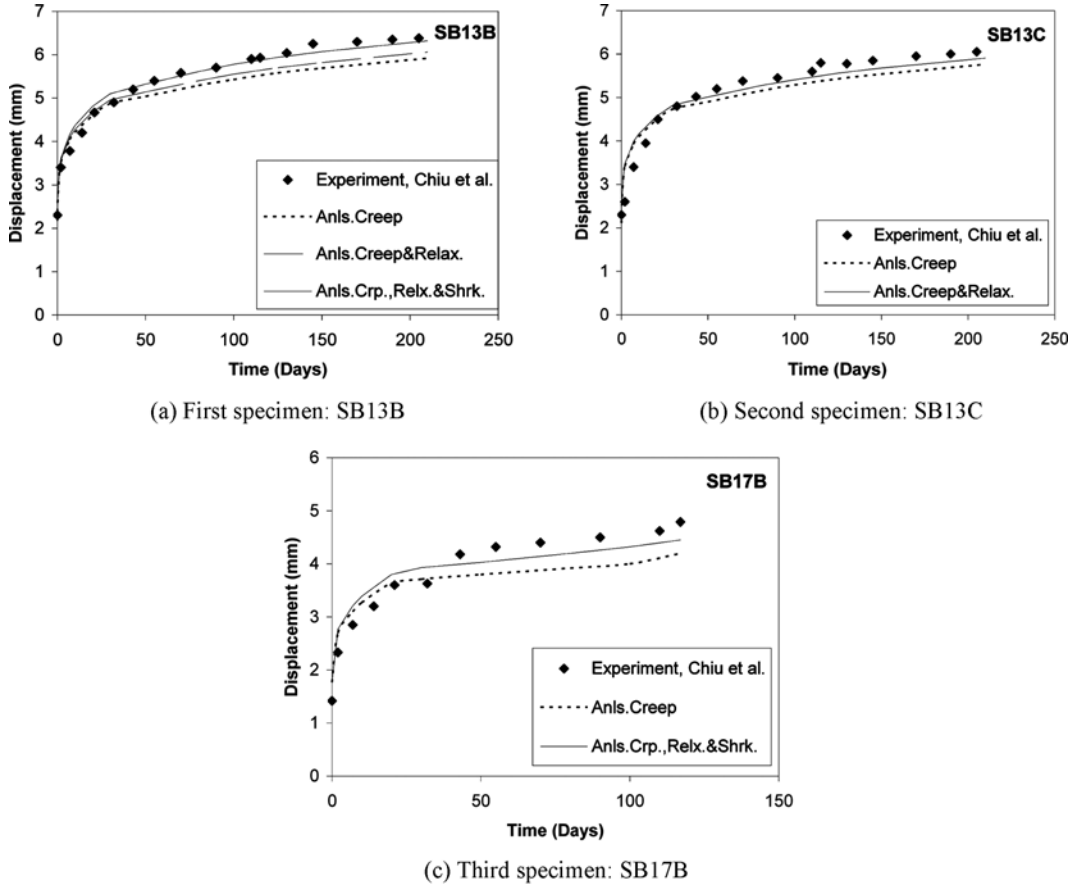

(a) First specimen: SB13B

(b) Second specimen: SB13C

(c) Third specimen: SB17B

Fig. 4 Comparison between experimental and analytical results: deflection at beam mid-span versus time

effects up to thirty years are also investigated by performing nonlinear analysis up to failure.

A typical span of 76.2 m consists of twenty 3.66-m-length precast box-girder segments and one 3-m-length cast-in-place key segment. Precast segments are considered to be assembled and prestressed at the age of twenty days after they are cast. At every other day, one segment is placed and pretensioned. After assembling the tenth segment on each side of the pier, a key segment is concreted. Then, continuity prestressing cables are tensioned to provide span continuity. Then, the superimposed loads, including the asphalt layer and bridge barriers, are applied. The software is then instructed to determine the time-dependent behaviour of the completed bridge up to thirty years. The bridge cross-sections considered in this analysis are made of a single-cell box girder with forty cantilever tendons and eight (for MSB1) or ten (for MSB2) continuity prestressing cables. Each cantilever tendon consists of 20, 12.7-mm-diameter strands, with cross-section area of 1974.19 mm^2, which are located in the deck slab. Each continuity cable consists of 9, 12.7-mm-diameter strands, with cross-section area of 888.38 mm^2, in MSB1 and 12, 12.7-mm-diameter strands, with cross-section area of 1184.51 mm^2, in MSB2 which are located in the webs, adjacent to bottom flange. All tendons are stressed to 1300 MPa, anchored with an anchor slip of 6 mm, and have a wobble friction coefficient, K_{wf}, of 0.0013 /m and a curvature friction coefficient, μ_{cf}, of 0.25/radian.

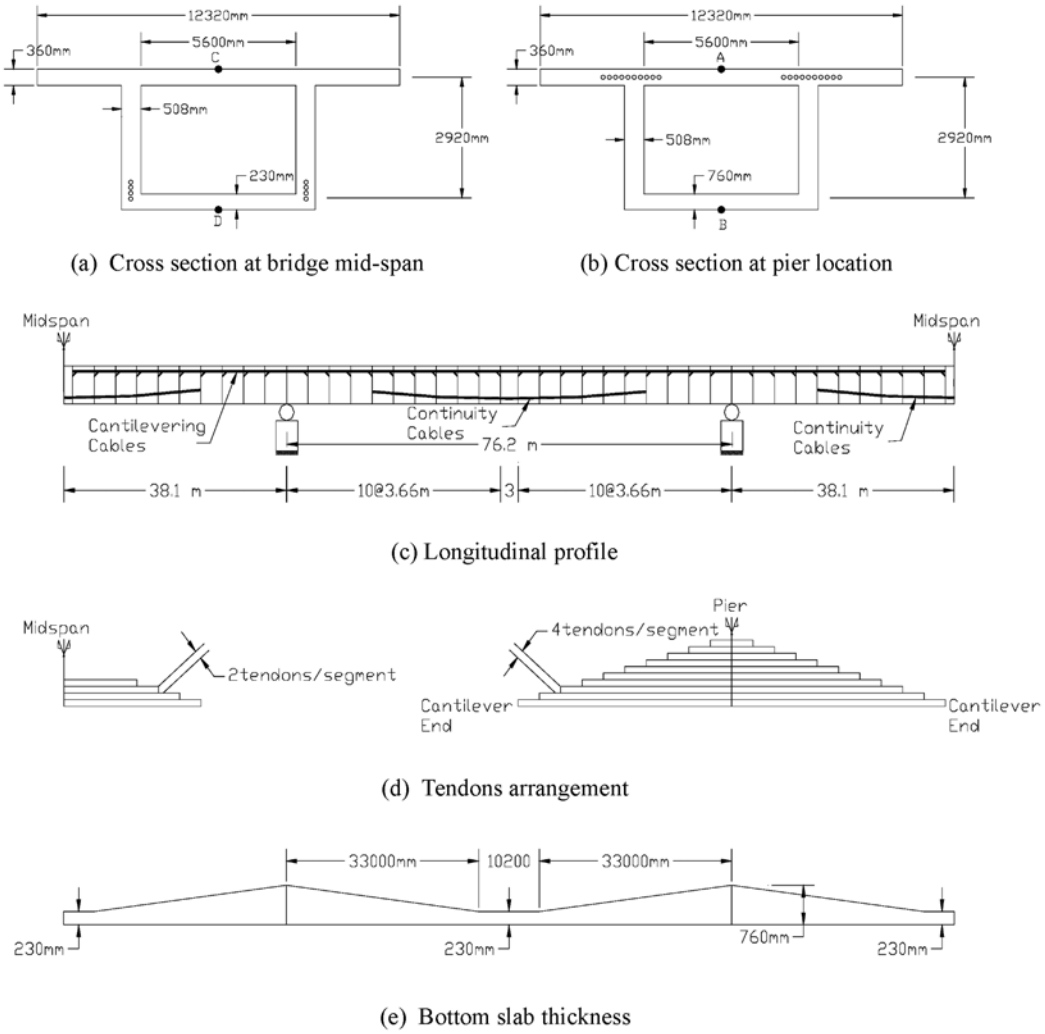

Fig. 5 Bridge geometry and tendons layout for MSB1

The concrete compressive strength, f_c', is 35 MPa, ultimate creep coefficient, ϕ_∞, is 3, ultimate shrinkage strain, $\varepsilon_{S\infty}$, is 0.0008 and unit weight, ρ, is 2400 kg/m^3. The prestressing steel has an elastic modulus, E_{ps}, of 193,000 MPa, ultimate strength, f'_{us}, of 1900 MPa, and relaxation coefficient, R, of 10.

The MSB1 bridge system shown in Fig. 5, consists of a constant depth deck girder with total depth of 3.48 m over the full length of the span, but MSB2 bridge shown in Fig. 6, is haunched, with a 3.48-m depth over the piers and 1.8 m depth at mid span. For the MSB2 bridge system, the depth of the girder at any point is of the form of the following equation:

$$d = a_0 \cdot x^{1.7} + d_0 \tag{12}$$

Where x is the distance from mid-span, d is the girder depth at location x both in mm, and a_0 and d_0

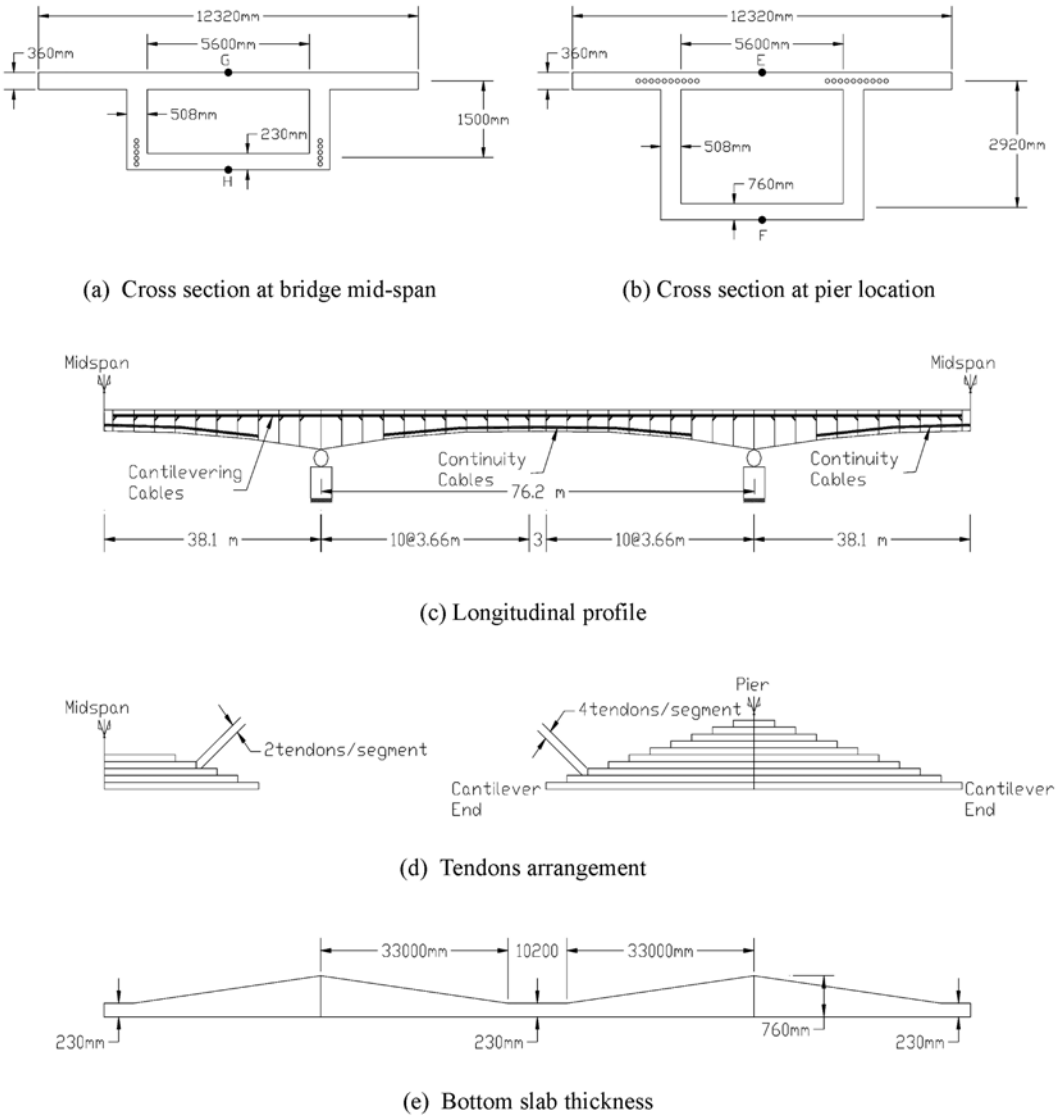

Fig. 6 Bridge geometry and tendons layout for MSB2

are constants equal to 27.4E-6 and 1800, respectively. The reinforcing steel is considered uniformly distributed on the bridge cross-section with an amount of 0.02 percent of the concrete area. The bottom slab thickness is also variable as shown in Figs. 5(e) and 6(e). More details about these examples can be found elsewhere (Ketchum and Scordelis 1986).

The construction period for each single span is according to the following sequence which starts after the piers are built:

- Days 0 to 20 : Casting of precast segments.
- Days 20 to 40 : Assembling of ten cantilever segments and placing and stressing cantilever tendons at a rhythm of one set every other day.

- Days 40 to 47 : Casting and curing of the keying segment at mid span.
- Days 47 to 50 : Placing and stressing continuity tendons.
- Days 50 to 75 : Placing pavement and railings (superimposed loads).

After verifying the modeling of time-dependent changes, two finite-element computer models are constructed, using the ABAQUS software, for bridges MSB1 and MSB2, respectively, to simulate stages of the construction as well as the time-dependent effects due to creep and shrinkage of concrete, relaxation of prestressing steel, changes in concrete properties with time, and change in the bridge structural system from statically determinate to statically indeterminate. All the short-term effects including prestress losses due to friction, anchorage slip, and construction stages are also considered. Views of the finite-element models of part of the segmental bridges MSB1 and MSB2 are shown in Fig. 7.

Fig. 8 shows the final displacement profile after putting all the segments in position for bridge MSB1. Only half of the cantilever system is illustrated because of symmetry. Values of deflection are intentionally presented due to segment self-weight only, due to prestressing effect only and finally for both self-weight and prestressing effects. These illustrate the level of the contribution of

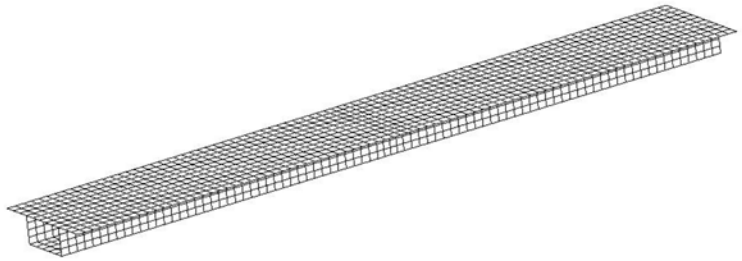

(a) Bridge MSB1

(b) Bridge MSB2

Fig. 7 Views of the finite-element modeling of the investigated bridges

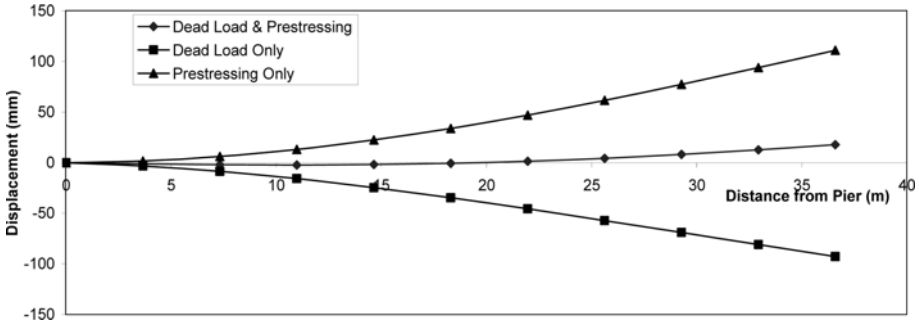

Fig. 8 Deflection of the bridge deck due to different loads for MSB1

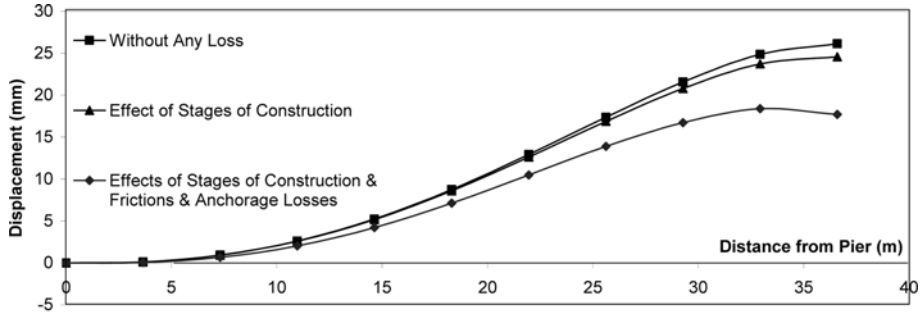

(a) Cantilever tips during construction

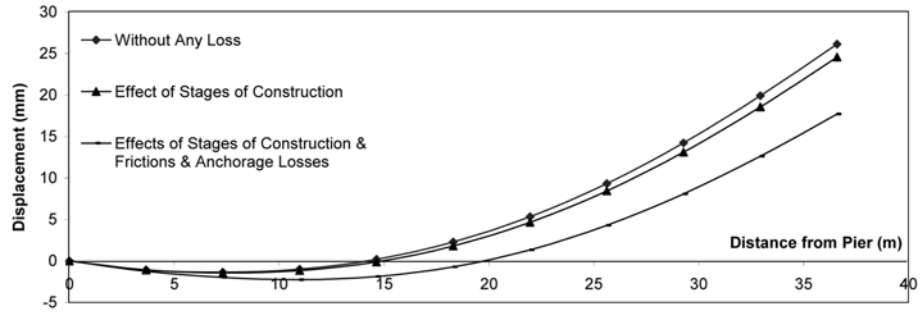

(b) At the end of cantilevering

Fig. 9 Deflection of the bridge deck due to short-term prestress losses for bridge MSB1

dead load as well as tendon prestressing to the global effect. It should be noted that the instantaneous losses due to friction and anchorage slip and elastic shortening of segments are included in the analysis at each time step. Fig. 9(a) shows the deflection values at the cantilever tips during construction steps in bridge MSB1. While Fig. 9(b) depicts the deflected shape of the cantilever system at the end of cantilevering, due to instantaneous prestress losses. As an example, the deflection of the tip of segment No. 5 just after installation is 8 mm, while the deflection at the same location becomes 3 mm after installing all the ten segments. It can also be observed that the losses due to the effects of the stage-by-stage construction process are much less than those due to friction and anchorage slip losses. Figs. 10(a) and 10(b) compare the effects of different time-dependent losses on the deflection of bridge segments during construction and after installing all the segments, respectively. It can be observed that all those time-dependent material deformations, including creep and shrinkage of concrete and relaxation of prestressing steel, have a significant effect on bridge deflection either during the construction stages or at the end of cantilevering. This type of analysis can be used to determine camber requirements during construction. For long-term deformation, it is obvious that the creep of concrete has the most significant effect on the behavior of the cantilever deck. For example, after placing the fifth segment, the deflection of the cantilever tip is 7.12 mm, when no time-dependent effect is considered and is 11.03, 10.85 and 10.36 mm when only the creep effect, creep and shrinkage effects and creep and relaxation effects, respectively, are included.

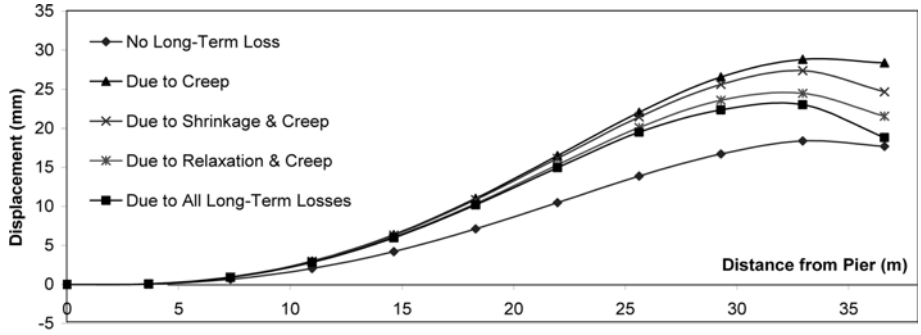

(a) Cantilever tips during construction

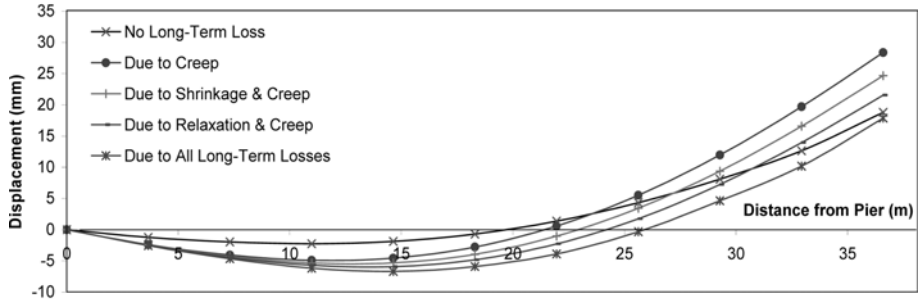

(b) At the end of cantilevering

Fig. 10 Deflection of the bridge deck due to time-dependent effects for bridge MSB1

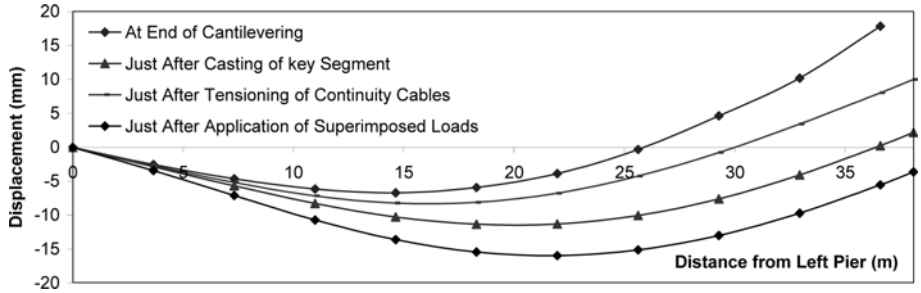

Fig. 11 Deflected shape of half-span of the MSB1 before and after installing continuity cables

After the two cantilevers from adjacent piers, of total length of 73.2 m, are erected, they are jointed together with a cast in place key segment of length 3 m. Then, continuity cables are placed and tensioned. Superimposed loads, including pavement, asphalt, and railing weights are applied at the end of construction process. These construction stages are simulated using ABAQUS software at different time steps. Fig. 11 depicts deflection of the bridge deck due to these different stages of construction for bridge MSB1. It can be observed that the mid-span upward deflection is reduced by 40% after introducing the keying segment and tensioning the continuity cables. By application of the superimposed load, the bridge deck exhibits downward deflection over its entire length.

Long-term deformations still exist after completion of the bride superstructure. The deflection

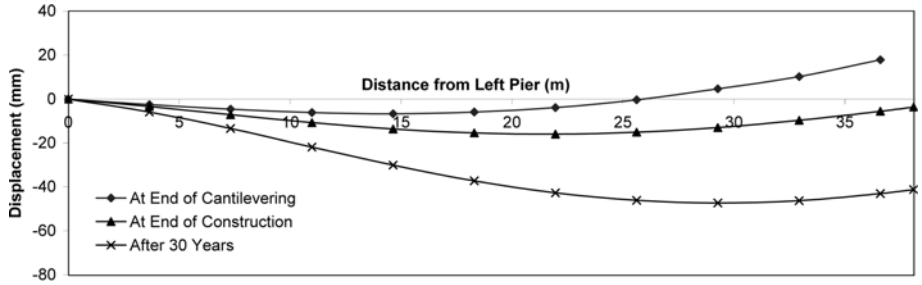

(a) Bridge MSB1

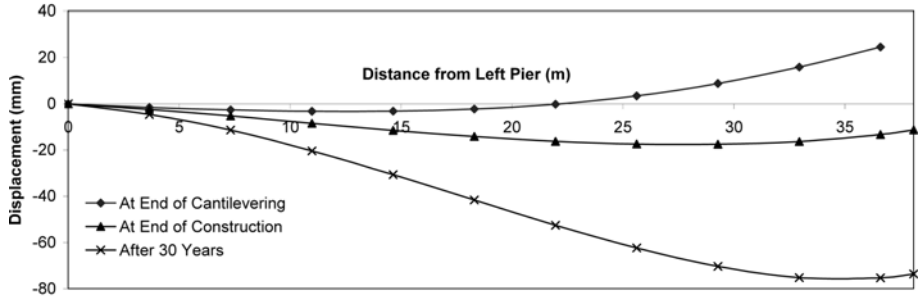

(b) Bridge MSB2

Fig. 12 Deflection profile at different stages of construction for bridges MSB1 and MSB2

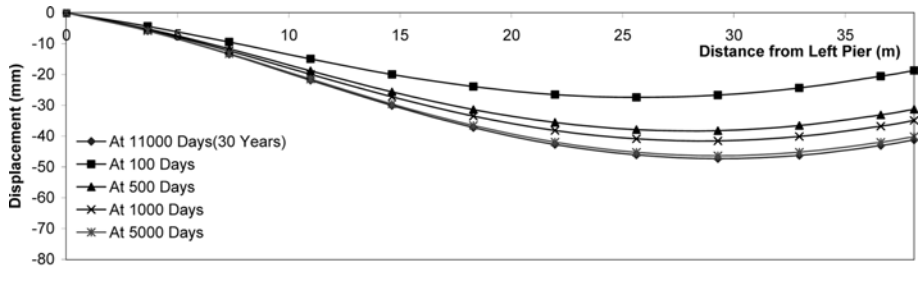

(a) Bridge MSB1

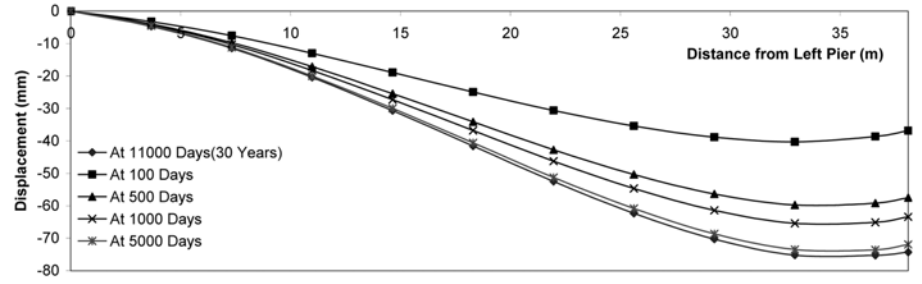

(b) Bridge MSB2

Fig. 13 Deflection profile for different ages for bridges MSB1 and MSB2

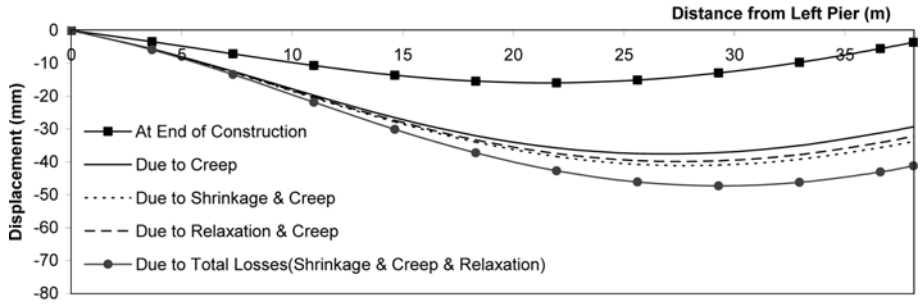

(a) Bridge MSB1

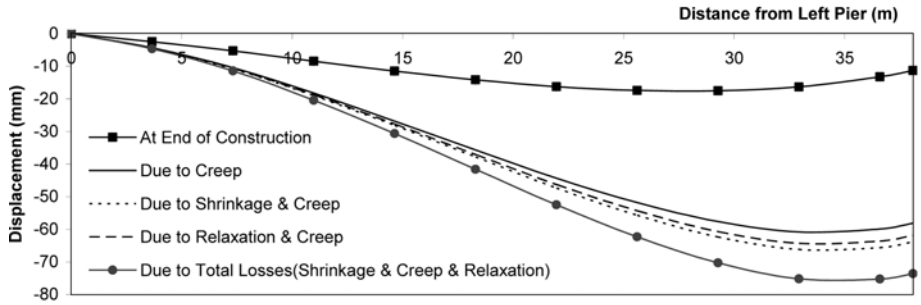

(b) Bridge MSB2

Fig. 14 Deflection profile due to different long-term effects after 30 years for bridges MSB1 and MSB2

profile of the half-span of bridges MSB1 and MSB2 at the end of cantilevering, at introducing continuity of bridge spans, and after 30 years of construction are shown in Fig. 12. While Fig. 13 depicts the increase in bridge deflections with time up to 30 years. In bridge MSB1, it can be observed that the deflections at the mid-span changes from 3.6 mm at the end of construction, to the 41.2 mm after 30 years. A similar observation can be made for bridge MSB2, but with bigger deflection values. Fig. 13 also shows that the rate of increase of long-term deformation decreases with time. Fig. 14 illustrates the deflected shape of the half-span of the bridges under the influence of the long-term effects of creep and shrinkage of concrete and the relaxation of prestressing steel. It can be observed that most of this deflection is due to the creep of concrete when compared to the contribution of concrete shrinkage and the relaxation of prestressing steel. Table 1 shows the variation of external (static) and internal bending moment at support location and at mid-span of the

Table 1 Variation of the bending moment of bridges MSB1 and MSB2

Bridge	Time	Static moment (MN·m)		Internal moment (MN·m)	
		At support	At mid span	At support	At mid span
MSB1	At end of construction	–175.07	16.02	–60.01	2.33
	After 30 years	–176.92	19.71	–74.64	7.82
MSB2	At end of construction	–160.0	16.70	–45.30	3.92
	After 30 years	–167.1	19.82	–65.21	7.05

Table 2 Variation of longitudinal stresses on bridge cross-section at pier location and mid-span of bridges MBS1 and MBS2

Time	Stress at point (MPa)				Stress at point (MPa)			
	A	B	C	D	E	F	G	H
At end of cantilevering	–5.05	–9.96	-	-	–6.42	–8.72	-	-
Before application of superimposed loads	–4.30	–10.10	0.01	–1.40	–5.29	–8.49	–0.59	–1.18
At end of construction	–2.98	–11.70	–0.72	–0.12	–3.96	–10.46	–1.67	0.33
After 30 years	–0.01	–11.18	0.07	2.30	–0.72	–10.49	–1.09	3.16

Note: For locations of points A to H, see Figs. 5 and 6.

bridges MSB1 and MSB2, at the end of construction and after 30 years of completion. The internal moment of the bridge is derived from internal in-plane forces in the shell elements forming the bridge cross-section. It can be noted that the influence of time-dependent effects on bending moments is not as pronounced as for deflections, especially for static moments. Top and bottom slab stresses at mid-span and pier locations of bridges MSB1 and MSB2 are shown in Table 2. Changes of stresses at different stages of construction and redistribution of stresses with time are observed and shown to be more pronounced at mid-span.

In order to study the behavior of the bridges MSB1 and MSB2 at the ultimate stage, a material nonlinear analysis is performed. For this purpose, bridges MSB1 and MSB2 are analyzed for live load effects according to the Canadian Highway Bridge Design Code, (CHBDC 2000), CHBDC specifies a uniformly distributed live load of 9 kN/m and 80% of the gross weight of a 625 kN truck in each lane, both at the end of construction and at thirty years old after construction. Fig. 15 shows view of this CHBDC lane loading. It should be noted that a CHBDC lane loading is considered in each of the two traveling lanes. Also, the resultant of the CHBDC lane loading is located at the mid-span point in such a way to produce the maximum mid-span moment. Simulation of the construction process is followed by the application of the CHBDC lane loading, which is incremented progressively up to failure just after construction and after thirty years. Fig. 16 shows load-deflection curves for the mid-span deflection with increase of live load. To simplify the presentation of the results, the vertical axes in Fig. 16 presents a fraction of the CHBDC lane

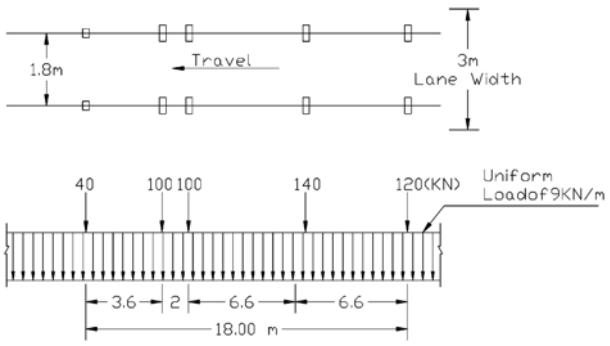

Fig. 15 CHBDC lane loading

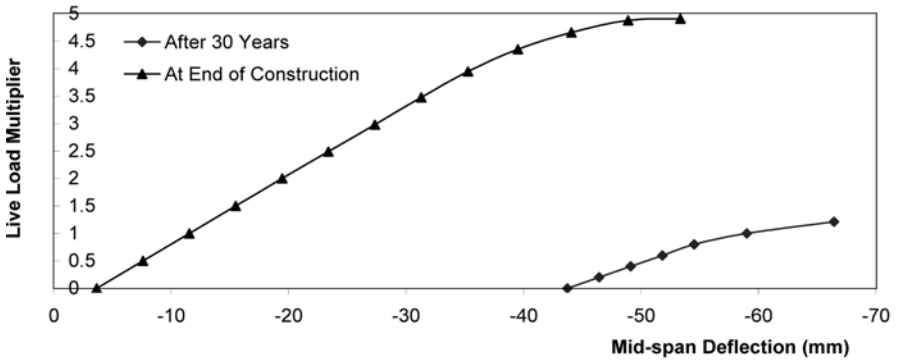

(a) Bridge MSB1

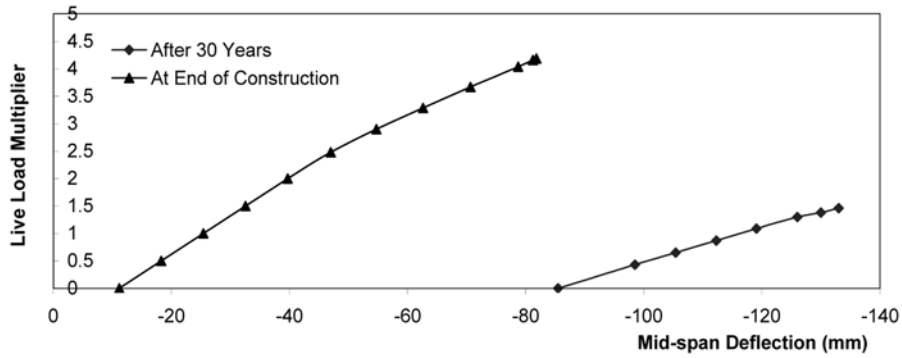

(b) Bridge MSB2

Fig. 16 Mid span deflection due to CHBDC live load

loading that can be carried by the bridge just at failure. This fraction is called "live load multiplier" herein. For MSB1 bridge, it is observed that cracks started at a high load increment at which a reduction of stiffness of the structures is observed. It is also observed that, failure occurs due to the propagation of cracks and the yielding of the continuity cables at mid-span. Fig. 16(a) shows that the ultimate load carrying capacity of bridge MSB1 decreases significantly after thirty years of construction as a result of time-dependent effects. It is remarkable that a live load factor (live load multiplier in Fig. 16) of 4.91 at the end of construction is reduced to 1.23 after thirty years of construction. Similar behavior is observed for bridge MSB2 at the end of construction, when it is subjected to increasing the CHBDC lane loading, as shown in Fig. 16(b). It can be observed that live load factor is 4.12 just after construction and 1.4 after thirty years of construction.

5. Conclusions

A general method for simulating the stages of construction and time-dependent analysis for segmental prestressed concrete box-girder bridges, built by the balanced-cantilever method, is proposed. A three-dimensional finite-element model is developed with the possibility to add and remove elements to change the statical system. Two typical bridges built by the balanced-cantilever

technique are analyzed using ABAQUS software. The structural behavior of the bridges under dead load and prestressing is traced throughout the construction phase and over a period of thirty years after construction. The analysis shows significant changes in the values of deflections, longitudinal stresses and internal forces as a result of long-term effects of creep and shrinkage of concrete and relaxation of the prestressing steel. Significant redistribution of stresses takes place at the mid span sections and at support locations, where only minor redistribution of static moments are observed in these cases. The short- and long-term ultimate load carrying capacity due to live load is also evaluated. It was also observed the ultimate load carrying capacity of such bridges decreases with time as a result of time-dependent effects.

Acknowledgements

This research is conducted through collaboration between Ryerson University of Toronto, Ontario, Canada, and Amirkabir University of Tehran, Iran.

References

ACI Committee 209. (1992), "Prediction of creep, shrinkage, and temperature effects in concrete structures", *American Concrete Institute Publication.*

Bazant, Z.P. (1972), "Prediction of concrete creep effects using age adjusted effective modulus method", *ACI J.*, **69**, 212-217.

Bishara, A.G. and Papakonstantinou, N.G. (1990), "Analysis of cast-in-place concrete segmental cantilever bridges", *J. Struct. Eng.*, ASCE, **116**, 1247-1268.

Bellevue, P.E. and Towell, P.J. (2000), "Creep and shrinkage effects in segmental bridges", *Advanced Technology in Structural Engineering,* SEI, ASCE, Philadelphia, Pennsylvania, USA, 1-8.

Canadian Standard Association. (2000), "Canadian highway bridge design code", CHBDC.CAN/CSA.S 6000, Etobicko, Ontario, Canada.

CEB – FIP, "Model code for concrete structures", 1978 and 1990.

Chiu, H.S., Chern, J.C. and Chang, K.C. (1996), "Long-term deflection control in cantilever prestressed concrete bridges, I and II", *J. Eng. Mech.,* ASCE, **122**, 489-501.

Cruz, P.J.S., Mari, A.R. and Roca, P. (1998), "Nonlinear time-dependent analysis of segmentally constructed structures", *J. Struct. Eng.,* ASCE, **124**, 278-287.

Dezi, L. and Tarantino, A.M. (1991), "Time dependent analysis of structures with a variable structural system", *J. of American Concrete Institute, ACI Mat. J.*, **88**, 320-324.

Dilger, W.H. (1982), "Creep analysis of pre-stressed concrete structures using creep-transformed section properties", *PCI J.*, **27**, 98-117.

Danon, J.R. and Gamble, W.L. (1977), "Time-dependent deformations and losses in concrete bridges built by the cantilever method", University of Illinois, Report No. UILU-ENG-77-2002.

Elbadry, M.M. and Debaiky, A.S. (1998), "Time-dependent stresses and deformations in segmentally erected curved concrete box-girder bridges", *Developments in Short and Medium Span Bridge Engineering'98,* CSCE, Calgary, AB, Canada, **2**, 399-412.

Floris, C., Marelli, R. and Regondi, L. (1991), "Creep effects in concrete structures: A study of stochastic behavior", *ACI Mat. J.*, **88**(3), 248-256.

Ghali, A. and Elbadry, M.M. (1989), "Serviceability design of continuous prestressed concrete structures", *PCI Journal.*

Gwozdziewicz, P., Jurkiewiez, B. and Destrebecq, J.F. (2000), "Long-term serviceability of concrete structures with regards to material behavior and cyclic loading", *Advanced Technology in Structural Engineering,* SEI,

ASCE, Philadelphia, Pennsylvania, USA, 1-8.
Hibbitt, H.D., Karlson, B.I. and Sorenson, E.P. (2004), "ABAQUS version 6.4, finite element program", Hibbitt, Karlson & Sorenson, Inc, Providence, R. I.
Kang, Y.J. and Scordelis, A.C. (1990), "Non-linear segmental analysis of reinforced and prestressed concrete bridges", *Developments in Short & Medium Span Bridge Engineering'90,* CSCE, Toronto, ON, Canada, **2**, 229-240.
Ketchum, M.A. and Scordelis, A.C. (1986), "Redistribution of stresses in segmentally erected prestressed concrete bridges", University of California, Berkeley, Report No. UCB/SESM-86-07.
Kwak, H.G. and Son, J.K. (2002), "Determination of design moments on bridges constructed by cantilever method", *J. Eng. Struct.,* Elsevier, **24**, 639-648.
Kwak, H.G., Seo, Y.J. and Jung, C.M. (2000), "Effects of the slab casting sequences and the drying shrinkage of concrete slabs on the short-term and long-term behavior of composite steel box girder bridges, Part 1 and 2", *J. Eng. Struct.,* Elsevier, **23**, 1453-1480.
Lefebvre, D. (2002), "Shrinkage and creep effects on pre-stressed concrete structures", *4th Structural Specialty Conf.,* CSCE, Montreal, Quebec, Canada.
Mari, A., Mirambell, E. and Estrada, I. (2003), "Effects of construction process and slab prestressing on the serviceability behavior of composite bridges", *J. Constructional Steel Research,* **59**, 135-163.
Mari, A.R. (2000), "Numerical simulation of the segmental construction of three dimensional concrete frames", *J. Eng. Struct.,* Elsevier, **22**, 585-596.
Melby, K., Jordet, E.A. and Hansvold, C. (1996), "Long-span bridges in Norway constructed in high strength LWA concrete", *J. Eng. Struct.,* Elsevier, **18**, 845-849.
Neville, A.M., Dilger, W.H. and Brooks, J.J. (1983), "Creep of plain and structural concrete", Longman, New York, USA.
Oh, B.H. and Yang, H. (2000), "Sensitivity analysis of time-dependent behavior in PSC box girder bridges", *J. Struct. Eng.,* ASCE, **126**, 171-179.
Ouellet, C. and Gaumond, Y. (1990), "Strengthening of two prestressed segmental box girder bridges", *Developments in Short & Medium Span Bridge Engineering'90,* CSCE, Toronto, ON, Canada, **2**, 259-269.
Robertson, I.N. (1998), "Instantaneous and long-term deflection of the North Halawa Valley Viaduct", *The East Asia-Pacific Conf. on Struc. Eng. & Cons.*, Taipei, Taiwan. **2**, 381-386.
Russell, H.G., Shiu, K.N., Gamble, W.L. and Marshall, V.L. (1982), "Measured and calculated time-dependent deformations in a post-tensioned concrete box girder bridge", *Int. Conf. on Short and Medium Span Bridge Engineering,* CSCE, Toronto, ON, Canada, **2**, 439-450.
Santos, L.O., Virtuoso, F. and Fernandes, J.A. (2001), "In situ measured creep and shrinkage of concrete bridges", *6th Int. Conf. on Creep, Shrinkage and Durability Mechanics of Concrete and Other Quasi-Brittle Materials*, Elsevier, M.I.T., Cambridge, USA.
Shushkewich, K.W. (1986), "Time-dependent analysis of segmental bridges", *Comput. Struct.,* **23**, 95-118.
Tadros, M.K., Ghali, A. and Dilger, W.H. (1979), "Long-term stresses and deformation of segmental bridges", *PCI Journal.*
Takacs, P.F. and Kanstad, T. (2001), "Short-time and long-time deformations of record span concrete cantilever bridges", *6th Int. Conf. on Creep, Shrinkage and Durability Mechanics of Concrete and Other Quasi-Brittle Materials*, Elsevier, M.I.T., Cambridge USA, **2**, 355-360.
Vanzyl, S.F. and Scordelis, A.C. (1979), "Analysis of curved prestressed segmental bridges", *J. Struct. Div.,* ASCE, **105**, 2399-2417.

Notation

a	: Correction factors for different conditions according to ACI 209
a_0	: Constant equal to 27.4E-6
b	: Correction factors for different conditions according to ACI 209
d	: Girder depth at location x (mm)
d_0	: Constant equal to 1800

E and E_i : Modulus of elasticity of concrete at different ages (MPa)
E_{ca} : Age-adjusted elastic modulus of concrete (MPa)
E_{ps} : Elastic modulus of prestressing steel (MPa)
E_s : Elastic modulus of steel (MPa)
f_p : Prestressing steel stress at time t (MPa)
f_{pi} : Initial stress of prestressing steel (MPa)
f_{py} : Yield stress of prestressing steel (MPa)
f_t : Tensile strength of concrete (MPa)
f'_{c28} : Compressive strength of concrete at 28 days (MPa)
$f'_c(t)$: Compressive strength of concrete at any time, t (MPa)
f'_{us} : Ultimate strength of prestressing steel (MPa)
G_{ca} : Age-adjusted shear modulus of concrete (MPa)
K_{wf} : Wobble friction coefficient (1/m)
l : Cantilever Length (m)
L : Span length (m)
M_t : Restraint moment after closure (N·mm)
P : Concentrated load (N)
q : Uniform load (N/m)
R : Relaxation coefficient for prestressing steel
t : Time of observation (days)
t_0 : Age of concrete at the end of initial wet curing in shrinkage calculations and age at initial loading in creep calculations (days)
t' : Age of concrete at application of variable loads (days)
x : Distance from mid span (mm)
α : Cantilever tip rotation (rad)
β_i (i = 1, 2, ...) : Correction factors for different conditions according to ACI 209
β_i' (i=1, 2, ...) : Correction factors for different conditions according to ACI 209
δ : Cantilever tip displacement (mm)
ε_r : Plastic strain
ε_s : Steel strain
$\varepsilon_{S\infty}$: Ultimate shrinkage strain
$\varepsilon_{s(t, t0)}$: Shrinkage strain of concrete at any time of, t
ε_y : Yield strain
ε_u : Ultimate strain
σ : Stress different ages (MPa)
σ_c : Concrete stress (MPa)
σ_y : Yield stress (MPa)
$\phi(t, t_0)$: Creep coefficient at any time of, t, for concrete loaded at the age of, t_0
$\phi(t_{k+1}, t_k)$: Creep coefficient in the period of (t_{k+1}, t_k)
ϕ_∞ : Ultimate creep coefficient of concrete
ρ : Unit weight of concrete (kg/m^3)
μ_{cf} : curvature friction coefficient (1/radian)
ν : Poisson's ratio
$\chi(t, t_0)$: Aging coefficient